

Article

Simple Microcontact Printing Technique to Obtain Cell Patterns by Lithography Using Grayscale, Photopolymer Flexographic Mold, and PDMS

Rocio Gimenez ^{1,†}, Camilo Pérez-Sosa ^{1,†}, Natalia Bourguignon ^{1,2,†}, Santiago Miriuka ³, Shekhar Bhansali ², Carlos R. Arroyo ⁴, Alexis Debut ⁴, Betiana Lerner ^{1,2,5,*} and Maximiliano S. Pérez ^{1,2,5,*}

¹ IREN Center, National Technological University, Buenos Aires 1706, Argentina

² Department of Electrical and Computer Engineering, Florida International University, Miami, FL 33174, USA

³ LIAN-CONICET-FLENI, Ruta 9 Km 52, 5, Belén de Escobar 1625, Argentina

⁴ Centro de Nanociencia y Nanotecnología, Universidad de las Fuerzas Armadas ESPE, Sangolqui P.O. Box 171-5-231B, Ecuador

⁵ Collaborative Research Institute Intelligent Oncology (CRIION), Hermann-Herder-Straße 4, 79104 Freiburg im Breisgau, Germany

* Correspondence: belerner@fiu.edu (B.L.); maxperez@fiu.edu (M.S.P.); Tel.: +54-11-4343-1177 (ext. 1209) (B.L.)

† These authors contributed equally to this work.

Citation: Gimenez, R.; Pérez-Sosa, C.; Bourguignon, N.; Miriuka, S.; Bhansali, S.; Arroyo, C.R.; Debut, A.; Lerner, B.; Pérez, M.S. Simple Microcontact Printing Technique to Obtain Cell Patterns by Lithography Using Grayscale, Photopolymer Flexographic Mold, and PDMS. *Biomimetics* **2022**, *7*, 155. <https://doi.org/10.3390/biomimetics7040155>

Academic Editor: Hermann Ehrlich

Received: 28 July 2022

Accepted: 5 October 2022

Published: 8 October 2022

Publisher's Note: MDPI stays neutral with regard to jurisdictional claims in published maps and institutional affiliations.



Copyright: © 2022 by the authors. Licensee MDPI, Basel, Switzerland. This article is an open access article distributed under the terms and conditions of the Creative Commons Attribution (CC BY) license (<https://creativecommons.org/licenses/by/4.0/>).

Abstract: Microcontact printing using PDMS embossing tools and its variations have aroused the interest of a wide spectrum of research fields, hence the feasibility of defining micro and nanoscale patterns. In this work, we have proposed and demonstrated a novel lithography method based on grayscale patterns printed in a flexographic photopolymer mold and transferred to epoxy resin and a single PDMS stamp to obtain different microprint pattern structures. The geometry of the patterns can be modified by adjusting the layout and grayscale of the stamp patterns. The functionality of this contact printing methodology was validated by generating human induced pluripotent stem cells (hiPSC) patterns. These specific micropatterns can be very useful for achieving complex differentiation in cell lines such as hiPSC. Microfabrication through the new technique provides a promising alternative to conventional lithography for constructing complex aligned surfaces; these structures could be used as components of biological patterns or microfluidic devices.

Keywords: grayscale; PDMS stamp; flexographic photopolymer mold; contact printing; 3D patterns

1. Introduction

Surface patterning has become an intensively researched area within material science and engineering [1]. A controlled topography can influence the optical [2], wetting [3,4], or adhesion properties [5,6] of a surface. Moreover, it has been exploited for a wide variety of applications that include superhydrophobic surfaces [7], smart windows [8], electronics [9], and biomedical purposes [10], among others. A wide range of technologies can be used to create these types of patterns, such as photolithography, surface wrinkling, soft lithography, microinjection molding, casting, and micro hot embossing.

Furthermore, an even more complex step is the creation of these patterns in three dimensions (3D), obtaining elements with different heights or shapes [11]. This type of complex micro and nanostructure can be achieved with technologies for modeling three-dimensional (3D) surfaces; grayscale lithography is one of the most known [12]. In grayscale lithography, the dose of ultraviolet light (UV) exposure is spatially modulated to locally control the crosslinking or dissolution rate of a material, generally a polymer or resin sensitive to ultraviolet (UV) rays. This material is used with grayscale masks [13–15]

or direct writing systems [16–18] to obtain structures with precise and arbitrary lateral and vertical dimensions.

Direct writing approaches typically involve expensive equipment that “writes” the design pixel by pixel, leading to low production speeds. These include Focus Ion Beam [19], Electron Beam [20], and Laser Lithography [21]. On the other hand, techniques that use physical gray tone masks can generally expose larger areas simultaneously, thus enabling mass production. However, the cost and time required to manufacture these masks hinder rapid prototyping, especially considering that a different mask is required for each pattern and that increasing the pattern’s complexity also increases the mask’s complexity. The main method for this approach is grayscale photolithography [14,22,23], while other lesser-known methods are based on X-ray [24] or holographic lithography [25].

Once these patterns are obtained on a surface, they can further function as molds or stamps to replicate the same design with other materials. A particularly suitable technique for this is microcontact printing (μ CP), which uses the relief pattern on the surface of a stamp to form patterns on the surfaces of substrates [26]. The stamp is ‘inked’ with a solution or material and brought into conformal contact with the surface of the substrate, transferring the ‘inked’ material only in the regions where the stamp makes contact with the substrate. This technique has been used to obtain arrays of nanoparticles [27], proteins [28], bacteria [29], and even DNA [30], thus, finding applications in biosensors, diagnostic immunoassays, chromatography, DNA microarrays, cell culturing, and further analytical procedures.

Previously, we reported and patented a simple and accessible process for the fabrication of polydimethylsiloxane (PDMS) microdevices by using a mold from a printing plate photopolymer called Flexcel as a master mold (Fmold) [31,32]. The Flexcel photopolymer enabled the transfer of these patterns to PDMS replicas with high reliability. The use of the Fmold allows the fabrication of master molds with dimensions up to 1270×2062 mm² and structure heights ranging from 53 to 1500 μ m [31]. This flexographic method presents advantages such as (a) low cost, (b) availability, (c) non-cleanroom facilities, (d) short time mold fabrication, (e) high durability of molds, (f) low surface roughness of the structures, and (g) the possibility of high-throughput production of epoxy resin molds and PDMS replicas with high precise replication [31,33]. Moreover, another previous work already reported the use of Fmold to create multilevel molds and then transfer the structures to PDMS replicas [34]. There, the different heights archived on the PDMS mold were controlled by modifying the UVA exposure time, so when the exposure time was longer, the height of the structure decreased, and vice versa. Herein, the novelty of the work is the manufacturing method based on photopolymers to create complex 3D patterns with a simple/basic grayscale mask using a Flexcel flexographic photopolymer. Unlike previously reported methods [31,33,34], the exposure time remained the same throughout the plate and the different heights present within the mold were archived by means of the grayscale mask. We show that a proper grayscale mask design is critical to fabricating pattern structures. The technology was validated using the pattern created on the PDMS surface as a template for microcontact printing in order to generate a respective pattern of human induced pluripotent stem cells (hiPSC) on the cell culture plates treated with reagents for adhesion.

2. Materials and Methods

2.1. Fabrication of PDMS Stamp

Figure 1 schematizes the manufacture of a PDMS stamp using a flexographic photopolymer-based manufacturing method that shows the main steps involved in the production of the photopolymer mold, the epoxy resin mold, and the PDMS replica.

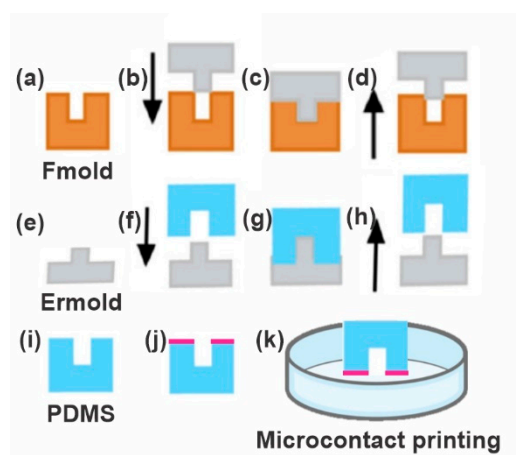


Figure 1. PDMS stamp fabrication. (a) Photopolymer flexographic master mold (Fmold). (b,c) The epoxy resin mold (ERmold) is formed on the Fmold and cured at room temperature. (d,e) The ERmold is demolded after 72 h. (f,g) The PDMS is cast on the ERmold and cured at 40 °C overnight. (h,i) The PDMS replica is peeled off. (j,k) The PDMS stamp is used for microcontact printing.

2.1.1. Photopolymer Flexographic Mold (Fmold)

The photopolymer Flexcel NX and Thermal Imaging Layer (TIL) in the fabrication of the molds were supplied by Eastman Kodak [35]. The photopolymer thickness was 1.14 mm. The grayscale mask was designed with Layout editor 20220423 software [36] using the amplitude modulated (AM) approach, a conventional screening technique that modifies the size of the dot but maintains the space between the dots fixed. The design was subsequently transferred to the TIL using an infrared laser source (2400 ppi), and then it was laminated onto the unexposed photopolymer plate. Following this step, the photopolymer plate was exposed to UVA light at 0.45 J on the reverse side, and then the front side was exposed to UVA light at 19 J for 360 s. The exposure to UVA wavelengths cross-links the organic compounds on the photopolymer plate. Subsequently, the TIL was removed. After UVA exposure, the photopolymer plate was washed with the solvent PRO-SOL N-1 (Eastman Kodak) at 360 mm/min and dried in an oven at 50 °C for 30 min. Lastly, the photopolymer plate was exposed to UVC light at 10 J for 17 min and UVA light on the front side at 4 J for 2 min. The UVC wavelengths are used to end the reaction, thus obtaining large, stable, and insoluble molecules. The photopolymer mold accordingly obtained was denominated Fmold [31,37].

2.1.2. Epoxy Resin Mold (ERmold)

Before creating the corresponding epoxy resin mold, the Fmold was placed in an oven for 12 h at 100 °C and then in a vacuum chamber for 1 h at room temperature. A cleaning process was then performed with 70% ethanol solution for 7 min in an ultrasonic bath, and later the Fmold was dried in an oven for 10 min at 40 °C. Finally, the Fmold was cleaned with a nitrogen stream. The epoxy resin and curing agent (Cristal-Tack, Novarchem-Argentina, Villa Martelli, Argentina) were mixed in a 2:1 wt ratio and gently stirred for 3 min. The mixture was sonicated (TESTLAB Ultrasonic Cleaner, Warsaw, Poland) to remove the air bubbles for 7 min. The epoxy resin was then slowly poured over the Fmold and cured for 72 h at room temperature. Finally, the epoxy resin mold (ERmold) was peeled off from the Fmold [33].

2.1.3. PDMS Stamp

Polydimethylsiloxane (PDMS) was mixed in a 10:1 wt ratio with a curing agent (Sylgard 184 Silicone Elastomer Kit, Germantown, WI, USA), as previously described in Peñaherrera et al. [38]. Subsequently, to remove air bubbles, the mixture was placed in a vacuum chamber for 30 min. Then, it was poured over the ERmold and cured overnight

in an oven at 40 °C. Next, the PDMS stamp was peeled off from the ER mold, and inlet and outlet holes were punched with a 1 mm diameter biopsy puncher (Integra Miltex® Ted Pella, Inc., Davies Drive, CA, USA).

2.2. Characterization

Before characterization, the PDMS stamp was blown with nitrogen gas to remove dust, followed by an ultrasonic bath in ethanol (70% *v/v*) for 10 min (repeated 5 times) and finally dried in an oven for 1 h at 40 °C. Morphological characterization was carried out using a Field Emission Gun Scanning Electron Microscope (TESCAN FEG SEM MIRA3, Brno, Czech Republic). The molds were previously metalized with a 20 nm gold layer, and SEM micrographs were taken at 5 kV to avoid damaging the samples. In addition, profilometry measurements were carried out with a Dektak XT profilometer from Bruker (Billerica, MA, USA). Linear scans were conducted at a scan speed of 22.75 $\mu\text{m/s}$ with a 25 μm radius tip and a sampling rate of 0.01 Hz/mm. The analysis was performed with Vision 64 software.

2.3. Cell Culture

Human induced pluripotent stem cells (hiPSC) were used. This cell line was modified to express a fluorescent protein (H2B-Cerulean), by means of the piggyBac method. The cell line was maintained in an E8 Flex medium (GIBCO), supplemented with Rock Inhibitor, in adherent cell culture plates functionalized with 1 \times Geltrex® (GIBCO, Waltham, MA, USA).

2.4. Contact Printing on Cell Culture Plates

To obtain the impression of the PDMS seal on the adherent culture plate, a chemical transfer methodology was used, mixing PEG (Polyethylene glycol 6000 SIGMA), PEGDA (Poly (ethylene glycol diacrylate) and a photoinitiator ((2-Hydroxy-4'-(2-hydroxyethoxy)-2-methylpropiophenone). For crosslinking on the surface, the three components were mixed until they formed a homogeneous substance. After this, the mixture was placed in a volume that completely covered the multiwell plate. To functionalize the crosslinking, the UV oven (UVP UltraViolet Crosslinker Model CI-1000, Upland, CA, USA) was used for 8 min at maximum intensity until evidencing the adherence of the mixture on the surface and the absence of lumps. After this, the seal was left overnight on the surface until the impression was completely transferred. Hoang, et al. [39], reported the concentrations and methodology in more detail used in this work.

3. Results and Discussion

The method of fabrication based on flexographic photopolymer molds used in this work [33] requires the use of a mask. Therefore, we designed and used a simple grayscale mask where one end is entirely opaque (blocks UV light) and gradually becomes more transparent (lets UV light pass through) (Figure 2A). To create this grayscale mask, we employed an array of dots of different sizes but with a fixed spacing, where the largest dots were located in the opaquer part of the mask, and vice versa.

As seen in Figure 2, we start from a relatively simple mask containing only squares of different gray tonalities (Figure 2A) to obtain a complex pattern of 3D structures (Figure 2D). Using the grayscale mask, we first obtain a pattern of dots in the photopolymer flexographic mold (Fmold) (Figure 2B) and a complementing structure in the epoxy resin mold (ER mold) (Figure 2C). Figure 2D shows the final PDMS stamps obtained with the 3D pattern of the design on their surface. The relief seen on PDMS replicas gradually varies in pattern and depth when viewed from one end of the stamp to the other (Figure 2D), replicating the pattern obtained in the Fmold.

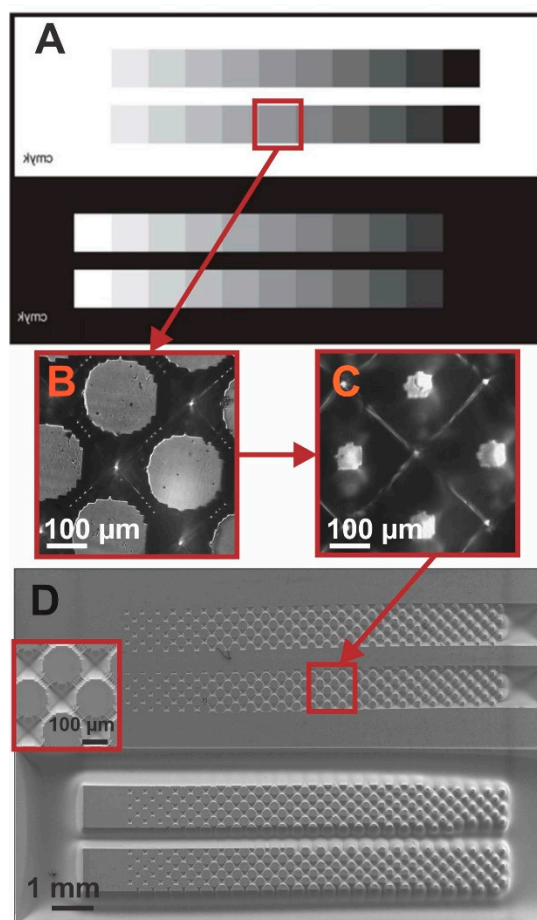


Figure 2. (A) Design of the grayscale mask used. (B) Optical image of the resulting pattern in the photopolymer flexographic mold (Fmold). (C) Optical image of the resulting pattern in the epoxy resin mold (ER mold). (D) SEM image of the PDMS stamp. The inset shows a magnification of the respective pattern obtained with the mask.

Figure 3A shows the SEM characterization of the forming patterns of circles obtained in the PDMS stamp which vary from smaller to larger diameters when going from a darker to a lighter grayscale, while the height is the same for all structures. Figure 3B shows profilometry profiles of the obtained 3D structures, where the depths of the cavities surrounding the circle patterns change from 10 μm to 150 μm . As seen in Figure 3A, on the right side of the stamp, we observe an array of dots, with diameters of approximately 100 μm , that are surrounded by cavities up to 130 μm deep. As one moves to the left side of the stamp, the dots begin to increase their size, gradually decreasing the space between them until finally, on the left side of the stamp, they interconnect, forming a network of dots. The depth of the cavities surrounding them also gradually diminishes until reaching a depth of 10 μm (Figure 3B). It should be noted that in the top image of Figure 2D and of Figure 3A we observe two pyramidal depressions that correspond to the black square of the grayscale mask. These depressions are observed instead of a pattern because the dots that should be formed are too small for the resolution of the technique, thus directly creating the depression. In addition, because the walls that are formed in this process are angled and not straight, the structure created has a pyramidal shape.

Our previous work already reported a flexographic photopolymer manufacturing method to create multilevel molds [34]. There, the different heights archived on the PDMS mold were controlled by modifying the UVA exposure time, so when the exposure time was longer, the height of the structure decreased, and vice versa. However, in the present work, the exposure time remained the same throughout the plate and the different heights present within the mold were archived by means of the grayscale mask.

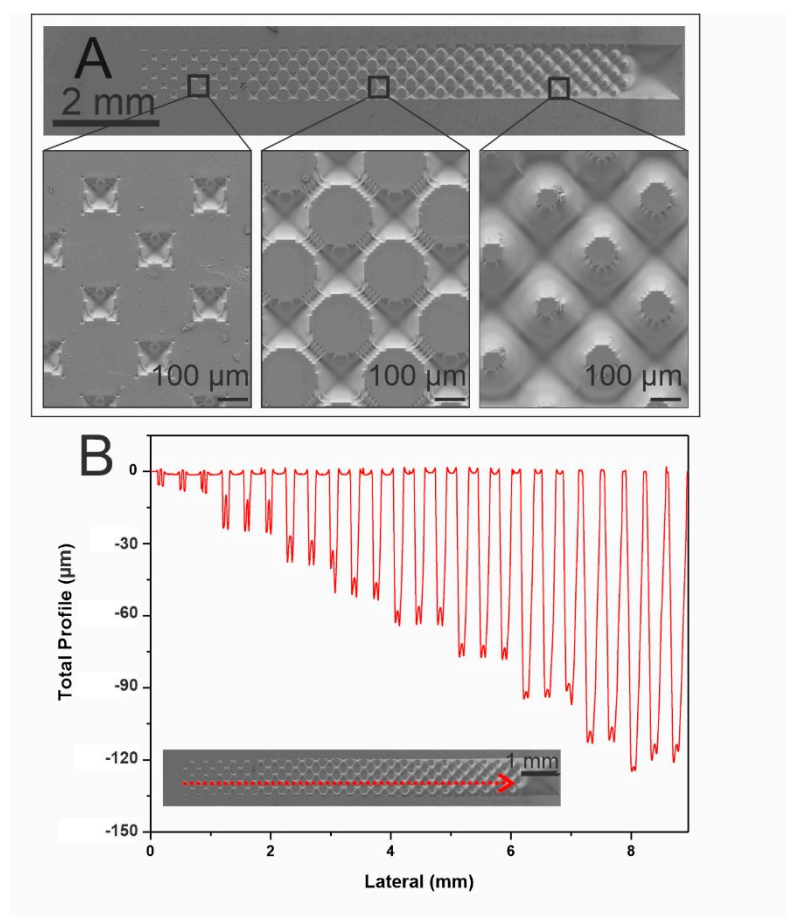


Figure 3. (A) SEM images of the 3D patterns of the PDMS stamp obtained from ERmold showing a magnification in three different areas. (B) profilometry profiles of the 3D structures of the PDMS replica obtained. Insert: SEM image shows the path on the structure profiled.

Using a grayscale mask with the conventional methods, such as photolithography and deep reactive ion etching, can generally obtain only basic reliefs such as ramps, which may even have limited resolution [22,40]. To achieve the same pattern that we obtained in this work using the traditional methods, the mask would have to be incredibly complex [41]. However, we were able to show that we can obtain this complex pattern using this simple mask, given the grayscale nature of the mask with dots of different sizes at a constant distance, in conjunction with the flexographic photopolymer fabrication method. Another difference observed with the photopolymer method is that the pattern obtained has the same height and cavities around it, whereas with the other methods, the reverse is typically obtained (i.e., the pattern has different heights). Moreover, by creating the PDMS mold from the ERmold that is a copy of the Fmold [31,33], we can obtain this type of inverse geometry.

Figure 3A shows the SEM characterization of the forming patterns of circles obtained in the PDMS stamp which vary from smaller to larger diameters when going from a darker to a lighter grayscale, while the height is the same for all structures. Figure 3B shows profilometry profiles of the obtained 3D structures of the PDMS replica, while the depths of the circle patterns change from 10 μm to 150 μm .

One of the main disadvantages of using an elastomeric stamp that exhibits high compressibility (Young's modulus ≈ 3 MPa [42]) is that it can collapse as a result of buckling or sticking laterally, for example [43]. This is especially true for stamps with high aspect ratios and can lead to defects on the pattern such as deviations in size and shape, or even printing in areas that must remain ink-free. However, a feature that can help avoid this type of drawback is that the stamp obtained in this work presents trapezoidal shapes,

especially perceptible in areas with high aspect ratios. In this manner, stamps manufactured with flexographic photopolymer, either using grayscale or conventional designs, would be suitable as stamps in structures with a high aspect ratio. It is also important to remark that by using this technique, we can generate these patterns in a single exposure in a large area ($1270 \times 2062 \text{ mm}^2$) as we reported for the Flexcel technique [31].

This embossed PDMS has subsequently used a stamp for microcontact printing to transfer molecules of interest with the desired pattern onto a surface. To generate cell patterns of human induced pluripotent stem cells (hiPSC), the cell culture plates were functionalized by mixing PEG, PEGDA and photo initiator. For this, the reagents were mixed until a homogeneous mixture was obtained and the surface was activated by UV light. After that, the PDMS stamp with the 3D patterns obtained was placed on the surface for 6 to 8 hours. Once the process was finished, the PDMS stamp was removed from the functionalized surface, leaving the printed pattern. For the seeding of the hiPSCs, $1 \times$ Geltrex was added on the previously treated surface. The geltrex was left for 1 h and 10,000 cells per ml were seeded.

Figure 4A shows how the cells adhered to the parts of the pattern where the Geltrex could functionalize. The black circles without cells correspond to the design of the PDMS stamp. In Figure 4B, it can be seen how the cells continued in time, forming cell aggregates with a greater number of cells but maintaining the segment of the pattern previously printed by the PDMS stamp.

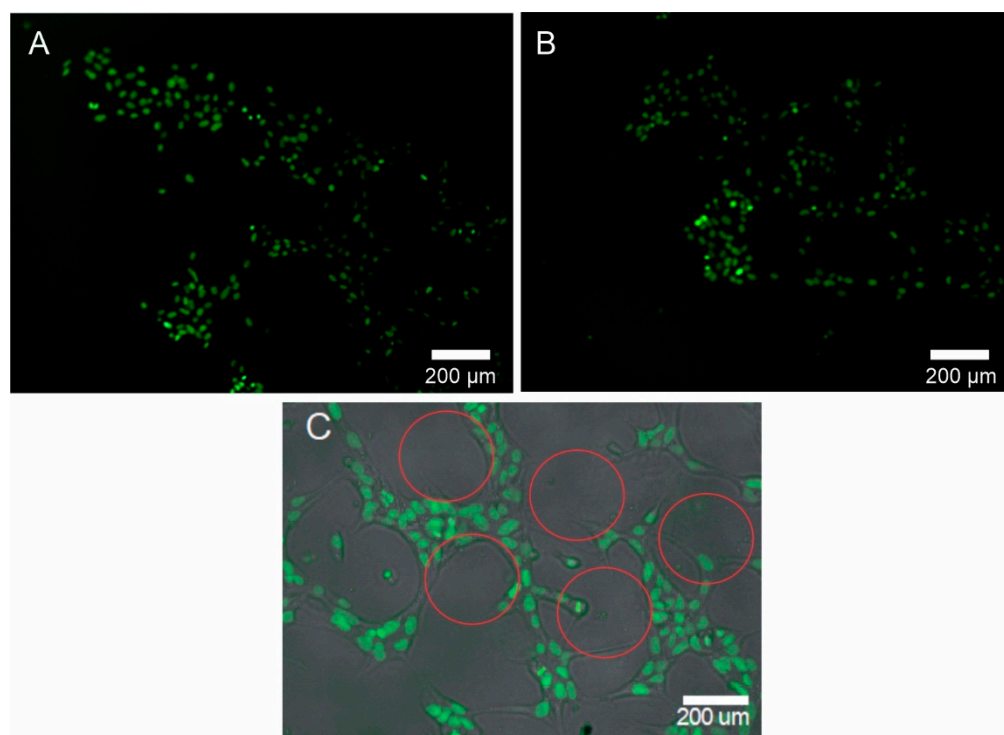


Figure 4. (A) Adhered hiPSC cells in the pattern printed on the culture plate. (B) Cells attached to a pattern of different heights with higher cell densities after 12 h of incubation. (C) Brightfield and overlay layer that show how the cells follow only the segment where the pattern was printed. Red outlines show the dots of the patterns created by the microcontact printing technique; the cells grew around the dots.

Microcontact printing (μ CP) can be very useful in the biological field to create patterns that allow achieving complex differentiation in cell lines such as hiPSC. It is known in advance that the surface is mainly responsible for biological performance [44]. The extracellular matrix is directly responsible for the signals emitted by cells which regulate cell behavior and fate [45]. Adding to micropattern technology, μ CP tools generate promising alternatives to improve the biological performance of many experiments associated with

cell culture and differentiation events, gene expression, and extracellular communication, among others [44]. In the present work, we demonstrate a simple and inexpensive system to be able to generate a μ CP that produces patterns for cell cultures in the hiPSC line.

4. Conclusions

We successfully demonstrated the fabrication of a complex 3D pattern on the surface of PDMS molds using a single step with a grayscale mask and flexographic photopolymer mold. The Fmold method, in conjunction with a grayscale mask, allowed us to create this elaborate pattern in a cost- and time-effective manner. We then proved that the embossed mold could be effectively employed as a stamp using microcontact printing in order to replicate that pattern on cell culture plates with induced human induced pluripotent stem cells. This up-and-coming tool will facilitate differential differentiation in stem cells based on pattern changes on the growth surface.

This grayscale mask and Fmold lithographic approach can be used to create a variety of three-dimensional topographies and structures in a single high-resolution lithographic step while enabling high-throughput, larger area fabrication of structures than ever before reported, with rapid reconfiguration. The versatility of this technique allows for the rapid prototyping of micromolds and relief structures that can be incorporated into devices with chemical and biological applications, microfluidics, and microelectromechanical systems.

Author Contributions: Conceptualization, B.L. and M.S.P.; formal analysis, R.G., N.B., S.M. and M.S.P.; funding acquisition, S.B., B.L., and M.S.P.; investigation, R.G., C.P.-S., N.B., C.R.A. and A.D.; methodology, R.G., C.P.-S., C.R.A. and A.D.; resources, S.B.; supervision, B.L. and M.S.P.; validation, C.P.-S.; visualization, S.M., S.B. and M.S.P.; writing—original draft, R.G. and C.P.-S.; writing—review and editing, N.B., B.L. and M.S.P. All authors have read and agreed to the published version of the manuscript.

Funding: This research was funded by the National Scientific and Technical Research Council grant number: PIP 2021-2023 11220200101707CO, Agencia Nacional de Promoción Científica y Tecnológica (ANPCYT), Fondo para la Investigación Científica y Tecnológica (FONCYT) and the Biothera Foundation. Funding was also provided by the National Institute on Minority Health and Health Disparities of the National Institutes of Health under Pilot Award Number 800013656, Florida International University Research Center in Minority Institutions. The content is solely the authors' responsibility and does not necessarily represent the official views of the National Institutes of Health.

Institutional Review Board Statement: Not applicable

Data Availability Statement: Not applicable.

Acknowledgments: The authors are thankful for the contribution of the Mertelsmann Foundation gGmbH and for the financial support from NIH, CONICET, ANPCyT and the Biothera Foundation.

Conflicts of Interest: The authors declare no conflicts of interest.

References

1. Ray, B.L. Special Section: Special Section: *Science* (80-). **2018**, *362*, 763.
2. Lee, H.; Jeon, T.Y.; Lee, S.Y.; Lee, S.Y.; Kim, S.-H. Designing Multicolor Micropatterns of Inverse Opals with Photonic Bandgap and Surface Plasmon Resonance. *Adv. Funct. Mater.* **2018**, *28*, 1706664. <https://doi.org/10.1002/adfm.201706664>.
3. Aguilar-Morales, A.I.; Alamri, S.; Voisiat, B.; Kunze, T.; Lasagni, A.F. The Role of the Surface Nano-Roughness on the Wettability Performance of Microstructured Metallic Surface Using Direct Laser Interference Patterning. *Materials* **2019**, *12*, 2737. <https://doi.org/10.3390/ma12172737>.
4. Li, Y.; Dai, S.; John, J.; Carter, K.R. Superhydrophobic surfaces from hierarchically structured wrinkled polymers. *ACS Appl. Mater. Interfaces* **2013**, *5*, 11066–11073. <https://doi.org/10.1021/am403209r>.
5. Wu, S.; Zhang, B.; Liu, Y.; Suo, X.; Li, H. Influence of surface topography on bacterial adhesion: A review. *Biointerphases* **2018**, *13*, 060801. <https://doi.org/10.1116/1.5054057>.
6. Geim, A.K.; Dubonos, S. V.; Grigorieva, I. V.; Novoselov, K.S.; Zhukov, A.A.; Shapoval, S.Y. Microfabricated adhesive mimicking gecko foot-hair. *Nat. Mater.* **2003**, *2*, 461–463.
7. Martines, E.; Seunarine, K.; Morgan, H.; Gadegaard, N.; Wilkinson, C.D.W.; Riehle, M.O. Superhydrophobicity and superhydrophilicity of regular nanopatterns. *Nano Lett.* **2005**, *5*, 2097–2103. <https://doi.org/10.1021/nl051435t>.

8. Li, Z.; Zhai, Y.; Wang, Y.; Wendland, G.M.; Yin, X.; Xiao, J. Harnessing Surface Wrinkling-Cracking Patterns for Tunable Optical Transmittance. *Adv. Opt. Mater.* **2017**, *5*, 1700425. <https://doi.org/10.1002/adom.201700425>.
9. Kim, D.; Ko, Y.; Kwon, G.; Kim, U.J.; You, J. Micropatterning Silver Nanowire Networks on Cellulose Nanopaper for Transparent Paper Electronics. *ACS Appl. Mater. Interfaces* **2018**, *10*, 38517–38525. <https://doi.org/10.1021/acsami.8b15230>.
10. Raghavan, S.; Chen, C.S. Micropatterned Environments in Cell Biology. *Adv. Mater.* **2004**, *16*, 1303–1313. <https://doi.org/10.1002/adma.200400594>.
11. Waheed, S.; Cabot, J.M.; Macdonald, N.P.; Lewis, T.; Guijt, R.M.; Paull, B.; Breadmore, M.C. 3D printed microfluidic devices: Enablers and barriers. *Lab Chip* **2016**, *16*, 1993–2013. <https://doi.org/10.1039/c6lc00284f>.
12. Lima, F.; Khazi, I.; Mescheder, U.; Tungal, A.C.; Muthiah, U. Fabrication of 3D microstructures using grayscale lithography. *Adv. Opt. Technol.* **2019**, *8*, 181–193.
13. Chen, C.; Hirdes, D.; Folch, A. Gray-scale photolithography using microfluidic photomasks. *Proc. Natl. Acad. Sci. USA* **2003**, *100*, 1499–1504. <https://doi.org/10.1073/pnas.0435755100>.
14. Pang, Y.; Shu, Y.; Shavezipur, M.; Wang, X.; Mohammad, M.A.; Yang, Y.; Zhao, H.; Deng, N.; Maboudian, R.; Ren, T.L. 3D Stretchable Arch Ribbon Array Fabricated via Grayscale Lithography. *Sci. Rep.* **2016**, *6*, 1–8. <https://doi.org/10.1038/srep28552>.
15. Stavis, S.M.; Strychalski, E.A.; Gaitan, M. Nanofluidic structures with complex three-dimensional surfaces. *Nanotechnology* **2009**, *20*, 165302. <https://doi.org/10.1088/0957-4484/20/16/165302>.
16. Loomis, J.; Ratnayake, D.; McKenna, C.; Walsh, K.M. Grayscale lithography—automated mask generation for complex three-dimensional topography. *J. Micro/Nanolithography MEMS MOEMS* **2016**, *15*, 013511. <https://doi.org/10.1117/1.jmm.15.1.013511>.
17. Grushina, A. Direct-write grayscale lithography. *Adv. Opt. Technol.* **2019**, *8*, 163–169. <https://doi.org/10.1515/aot-2019-0024>.
18. Mortelmans, T.; Kazazis, D.; Guzenko, V.A.; Padeste, C.; Braun, T.; Stahlberg, H.; Li, X.; Ekinici, Y. Grayscale e-beam lithography: Effects of a delayed development for well-controlled 3D patterning. *Microelectron. Eng.* **2020**, *225*, 111272. <https://doi.org/10.1016/j.mee.2020.111272>.
19. Erdmanis, M.; Tittonen, I. Focused ion beam high resolution grayscale lithography for silicon-based nanostructures. *Appl. Phys. Lett.* **2014**, *104*, 073118. <https://doi.org/10.1063/1.4866586>.
20. Schleunitz, A.; Schiff, H. Fabrication of 3D patterns with vertical and sloped sidewalls by grayscale electron-beam lithography and thermal annealing. *Microelectron. Eng.* **2011**, *88*, 2736–2739.
21. Gale, M.T. Fabrication of continuous-relief micro-optical elements by direct laser writing in photoresists. *Opt. Eng.* **1994**, *33*, 3556. <https://doi.org/10.1117/12.179892>.
22. Mosher, L.; Waits, C.M.; Morgan, B.; Ghodssi, R. Double-exposure grayscale photolithography. *J. Microelectromech. Syst.* **2009**, *18*, 308–315. <https://doi.org/10.1109/JMEMS.2008.2011703>.
23. Abdul Hamid, I.S.L.; Khim, B.K.; Sal Hamid, S.; Abd Rahman, M.F.; Abd Manaf, A. Implementation of a single emulsion mask for three-dimensional (3D) microstructure fabrication of micromixers using the grayscale photolithography technique. *Micromachines* **2020**, *11*, 548. <https://doi.org/10.3390/MII11060548>.
24. Mekaru, H. Fabrication and evaluation of a grayscale mask for x-ray lithography using MEMS technology. *J. Micro/Nanolithography MEMS MOEMS* **2008**, *7*, 013009. <https://doi.org/10.1117/1.2894817>.
25. Shrauger, V.E.; Erwin, L.L.; Ahn, J.L.; Warde, C. Computer-generated multiple-phase-level holograms by use of color-printer techniques. *Appl. Opt.* **1994**, *33*, 5318. <https://doi.org/10.1364/ao.33.005318>.
26. Kaufmann, T.; Ravoo, B.J. Stamps, inks and substrates: polymers in microcontact printing. *Polym. Chem.* **2010**, *1*, 371–387.
27. Santhanam, V.; Andres, R.P. Microcontact Printing of Uniform Nanoparticle Arrays. *Nano Lett.* **2004**, *4*, 41–44. <https://doi.org/10.1021/nl034851r>.
28. Bernard, A.; Renault, J.P.; Michel, B.; Bosshard, H.R.; Delamarche, E. Microcontact printing of proteins. *Adv. Mater.* **2000**, *12*, 1067–1070. [https://doi.org/10.1002/1521-4095\(200007\)12:14<1067::AID-ADMA1067>3.0.CO;2-M](https://doi.org/10.1002/1521-4095(200007)12:14<1067::AID-ADMA1067>3.0.CO;2-M).
29. Xu, L.; Robert, L.; Ouyang, Q.; Taddei, F.; Chen, Y.; Lindner, A.B.; Baigl, D. Microcontact printing of living bacteria arrays with cellular resolution. *Nano Lett.* **2007**, *7*, 2068–2072. <https://doi.org/10.1021/nl070983z>.
30. Lange, S.A.; Benes, V.; Kern, D.P.; Hörber, J.K.H.; Bernard, A. Microcontact Printing of DNA Molecules. *Anal. Chem.* **2004**, *76*, 1641–1647. <https://doi.org/10.1021/ac035127w>.
31. Bourguignon, N.; Olmos, C.M.; Sierra-Rodero, M.; Peñaherrera, A.; Rosero, G.; Pineda, P.; Vizuete, K.; Arroyo, C.R.; Cumbal, L.; Lasorsa, C.; et al. Accessible and Cost-Effective Method of PDMS Microdevices Fabrication Using a Reusable Photopolymer Mold. *J. Polym. Sci. Part B Polym. Phys.* **2018**, *56*, 1433–1442. <https://doi.org/10.1002/polb.24726>.
32. Bhansali, S.; Perez, M.S.; Lerner, B.; Bourguignon, N. Large Microfluidic Bioreactor And Manufacturing Method Thereof. U.S. Patent 11,135,589, 5 October 2021.
33. Olmos, C.M.; Vaca, A.; Rosero, G.; Peñaherrera, A.; Perez, C.; de Sá Carneiro, I.; Vizuete, K.; Arroyo, C.R.; Debut, A.; Pérez, M.S.; et al. Epoxy resin mold and PDMS microfluidic devices through photopolymer flexographic printing plate. *Sens. Actuators B Chem.* **2019**, *288*, 742–748. <https://doi.org/10.1016/j.snb.2019.03.062>.
34. Olmos, C.M.; Peñaherrera, A.; Rosero, G.; Vizuete, K.; Ruarte, D.; Follo, M.; Vaca, A.; Arroyo, C.R.; Debut, A.; Cumbal, L.; et al. Cost-effective fabrication of photopolymer molds with multi-level microstructures for pdms microfluidic device manufacture. *RSC Adv.* **2020**, *10*, 4071–4079. <https://doi.org/10.1039/c9ra07955f>.
35. Kodak Flexcel NX. Available online: <https://www.miraclon.com/products-technology/our-technology/> (accessed on 1 September 2022).
36. Layout Editor. Available online: <https://layouteditor.com/> (accessed on 1 September 2022)

37. Pérez-Sosa, C.; Pazmiño Peñaherrera, A.B.; Rosero, G.; Bourguignon, N.; Aravelli, A.; Bhansali, S.; Pérez, M.S.; Lerner, B. Novel Reproducible Manufacturing and Reversible Sealing Method for Microfluidic Devices. *Micromachines* **2022**, *13*, 650. <https://doi.org/10.3390/mi13050650>.
38. Peñaherrera, A.; Payés, C.; Sierra-Rodero, M.; Vega, M.; Rosero, G.; Lerner, B.; Helguera, G.; Pérez, M.S.S. Evaluation of cell culture in microfluidic chips for application in monoclonal antibody production. *Microelectron. Eng.* **2016**, *158*, 126–129. <https://doi.org/10.1016/j.mee.2016.03.059>.
39. Hoang, P.; Wang, J.; Conklin, B.R.; Healy, K.E.; Ma, Z. Generation of spatial-patterned early-developing cardiac organoids using human pluripotent stem cells. *Nat. Protoc.* **2018**, *13*, 723–737. <https://doi.org/10.1038/nprot.2018.006>.
40. Waits, C.M.; Morgan, B.; Kastantin, M.; Ghodssi, R. Microfabrication of 3D silicon MEMS structures using gray-scale lithography and deep reactive ion etching. *Sens. Actuators A Phys.* **2005**, *119*, 245–253. <https://doi.org/10.1016/j.sna.2004.03.024>.
41. Hamid, I.S.L.A.; Khim, B.K.; Omar, M.F.M.; Zain, K.A.M.; Rhaffor, N.A.; Hamid, S.S.; Manaf, A.A. Three-Dimensional Soft Material Micropatterning via Grayscale Photolithography for Improved Hydrophobicity of Polydimethylsiloxane (PDMS). *Micromachines* **2022**, *13*, 78. <https://doi.org/10.3390/mi13010078>.
42. Bietsch, A.; Michel, B. Conformal contact and pattern stability of stamps used for soft lithography. *J. Appl. Phys.* **2000**, *88*, 4310–4318. <https://doi.org/10.1063/1.1289816>.
43. Alom Ruiz, S.; Chen, C.S. Microcontact printing: A tool to pattern. *Soft Matter* **2007**, *3*, 168–177.
44. Qiu, S.; Ji, J.; Sun, W.; Pei, J.; He, J.; Li, Y.; Li, J.J.; Wang, G. Recent advances in surface manipulation using micro-contact printing for biomedical applications. *Smart Mater. Med.* **2021**, *2*, 65–73. <https://doi.org/10.1016/j.smaim.2020.12.002>.
45. Chen, L.; Yan, C.; Zheng, Z. Functional polymer surfaces for controlling cell behaviors. *Mater. Today* **2018**, *21*, 38–59. <https://doi.org/10.1016/j.mattod.2017.07.002>.